INDC INTERNATIONAL NUCLEAR DATA COMMITTEE

MEASUREMENT OF 14-MeV NEUTRON MULTIPLICATION FACTOR

IN SPHERICAL LEAD AND BISMUTH ASSEMBLIES BY

THE TOTAL ABSORPTION METHOD

V.M. Novikuv, D.Yu Chuvilin, V.A. Zagryadskij, M.I. Krajnev
D.V. Markovskij, G.E. Shatalov

I.V. Kurchatov Atomic Energy Institute
Moscow

MEASUREMENT OF 14-MeV NEUTRON MULTIPLICATION FACTOR

IN SPHERICAL LEAD AND BISMUTH ASSEMBLIES BY

THE TOTAL ABSORPTION METHOD

V.M. Novikuv, D.Yu Chuvilin, V.A. Zagryadskij, M.I. Krajnev
D.V. Markovskij, G.E. Shatalov

I.V. Kurchatov Atomic Energy Institute
Moscow

MEASUREMENT OF 14-MeV NEUTRON MULTIPLICATION FACTOR IN SPHERICAL LEAD
AND BISMUTH ASSEMBLIES BY THE TOTAL ABSORPTION METHOD

V.M. Novikuv, D.Yu Chuvilin, V.A. Zagryadskij, M.I. Krajnev,
D.V. Markovskij, G.E. Shatalov

I.V. Kurchatov Atomic Energy Institute

Moscow 1985

Abstract

This work is devoted to the neutron leakage measurement from
Pb and Bi sphere assemblier with help of the "boron tank" method
per one 14-MeV neutron. The neutron leakage from Pb assemblies
was compared with BLANK program calculations using ENDL nuclear
data. It was shown that discrepancy between calculations and
experiments was 0,065 ± 0,039 for 3 cm Pb thickness and
0,080 ± 0,047 for 9 cm Pb thickness. The conclusion is made,
that (n,2n) cross-section for Pb is greater than cross-section
using in BLANK program.

INTRODUCTION

In a number of designs for thermonuclear reactors, lead is
considered to be a suitable material for use in the blanket as a fusion
neutron breeder [1-3]. Such attention to this element is due to its
relatively high cross-section for the (n,2n) reaction, its very low
radiation capture cross-section and also its availability and
workability. Accuracy in predicting the design parameters of a
thermonuclear reactor blanket depends on the reliability of the nuclear
physics constants used in the calculations. The study of Youssef et al.
[4] analyses the sensitivity of a hybrid thermonuclear reactor (the
SOLASE-H project) to the constants of lead. The analysis showed that the
error of 4% in the determination of the ^{233}U conversion coefficient is
associated mainly with error in the cross-sections of reactions in lead.
It is shown that the coefficient of tritium-^6Li conversion is very
sensitive to the constants of lead.

However, considerable scatter of the data is found in the published studies on measurement of the cross-section for the (n,2n)-reaction in lead in the case of 14-MeV neutrons [5-9] (Table 1). This table also presents data for bismuth. This element is similar in its nuclear physics properties to lead and may also be considered a breeder of fusion neutrons. As will be seen from the table, the data for bismuth differ considerably from one another.

Recent years have seen the publication of the results of integral experiments in lead assemblies with 14-MeV neutron sources. In a study of V.D. Aleksandrov et al. [10], measurements were made of the activation reaction rates of threshold detectors inside spherical shells (inverse geometry). The source of 14-MeV neutrons was situated outside the spheres. The results, presented in the form of spatial indices, were compared with the calculations according to the BLANK program [11], in which the constants for lead from the ENDL library were used. The comparison showed that in the case of the indium and radium detectors, the calculated values of the indices were lower by a factor of 2 than the experimental values. For detectors with a higher threshold, the difference between the results was smaller and, starting with $E_{thr} = 5$ MeV, experiment and calculation coincide, within the limits of error.

Bogomolov et al. [12], using activated threshold detectors investigated a layered system of lead and polyethylene in a flat geometry. It was shown that in the lead zone the activation reaction rate for ^{115}In (n,n') was 40% higher than the calculated values obtained by the BLANK program.

A. Takahashi et al. [13] measured the leakage neutron spectrum by the time-of-flight method from four spherical lead shells. The 14-MeV neutron source was placed in the centre of the shells. The dimensions of the shells were: $R_{intern.} = 10$ cm for all spheres; the thickness of the shells was 3, 6, 9 and 12 cm. The experimental results of this study are presented in Table 2. M. Segev [14] presents an analysis of these experimental results and concludes that such extensive neutron multiplication as that obtained experimentally cannot be explained by the existing concept of nuclear physics constants in lead.

Thus, the attractiveness of using lead as a fusion neutron breeder, on the one hand, and the conflicting nature of the experimental data, on the other hand, induced authors to set up an experiment for measuring the efficiency of fusion neutron multiplication in the case of lead. At the same time, measurements were made for bismuth as well.

According to the study of S.A. Konakov et al. [15], indium and radium detectors are very sensitive to the shape of the secondary neutron spectrum. This means that the same number of secondary neutrons of the different shape of the spectrum, can make a markedly different contribution to the activation intervals of indium and radium detectors. Hence the theoretical and experimental differences for these detectors in Refs [10, 12] do not permit any definite conclusion to be drawn regarding the correctness of the (n,2n) cross-section from the ENDL library. To verify the rate of neutron multiplication in this reaction, it was decided to measure the absolute leakage of neutron by the "boron tank" method, with normalization to one neutron from a source. The finding

obtained with measurement by this method was that absolute neutron leakage depends mediately on the shape of the secondary neutron spectrum - through the possibility of additional multiplication in "direct" neutrons of the (n,n') reaction.

However, this dependence is very slight owing to the high threshold of the (n,2n) reaction ($\sim$ 7.5 MeV) and the comparatively small share of secondary neutrons from direct processes. Hence the main reason for the possible discrepancy between experiment and calculation for lead and bismuth assemblies in the measurement of absolute leakage by the "boron tank" method lies with the cross-section of the (n,2n) reaction. The reasoning behind the use of this method, its possibilities and advantages are described in the paper of V.A. Zagryadskij et al. [16].

1. SUMMARY OF THE METHOD

The assembly under study, which has the shape of a spherical shell, is placed at the centre of a large space, filled with a solution of boric acid in water. The source of 14-MeV neutrons is positioned at the centre of the assembly via a special channel. The neutrons emerging from the source and escaping into the water are slowed down, releasing energy lower than the threshold of the (n,2n) reaction. For this reason the reflected neutrons cannot give rise to supplementary multiplication. The boric acid solution is a good absorber of thermal neutrons and so prevents their flow into the assembly. For these reasons, as was shown in Ref. [16], the layer of borated water does not affect the leakage of neutrons from lead and bismuth assemblies. It is also shown in Ref. [16] that the rate of neutron capture by boron in the case of a sufficiently large tank is also independent of the initial neutron energy in the 0.01-6 MeV energy range. Since the spectrum of neutrons from the assembly consists of two components (14-MeV neutrons from the source and secondary, inelastic-interaction neutrons having an energy of $E \lesssim 6$ MeV) we can introduce a value proportional to the efficiency of neutron capture by boron for both of the components. For this purpose a measurement was made of the spatial distribution of the counting rate of the boron counter for the tank per one 14-MeV neutron without assemblies. This distribution was then integrated over the volume of the boron tank. Since the secondary neutrons can be modified by a ^{252}Cf source [16], a similar procedure was carried out for such a source.

Let us call a detector of total neutron absorption (TAD) a "boron tank". Having obtained values proportional to the efficiencies of such detectors for the case of 14-MeV neutrons and secondary inelastic-interaction neutrons, we carried out a similar procedure (measurement of the spatial distribution of the counting rate of a boron counter and its subsequent integration over the volume of a tank) with the assembly under study. We identify the neutrons from elastic scattering, which for all practical purposes do not lose energy on heavy elements, with neutrons from a 14-MeV source and write the equation:

$$N = \varepsilon_{14\ MeV}\ T + \varepsilon_{Cf}\ N_{sec}, \tag{1}$$

where N is the counting rate of a boron counter integrated over the volume of a "boron tank" containing the assembly under study; $\varepsilon_{14 \text{ MeV}}$ is a value proportional to the efficiency of a TAD for 14-MeV neutrons; T is a transmission function - the number of neutrons from a source passing through the assembly without interaction plus neutrons inelastically scattered by nuclei of the assembly; ε_{Cf} is a value proportional to the efficiency of the TAD for secondary inelastic-interaction neutrons; N_{sec} is the number of secondary inelastic-interaction neutrons in the assembly.

All the values in expression (1) were normalized in terms of one neutron from the source. The leakage of neutrons can be represented as follows:

$$M = T + N_{sec} \tag{2}$$

The value of T can be obtained by any supplementary methods (activation detectors, detectors for recoil protons etc.), if there is reason for considering the elastic-interaction cross-section to be sufficiently well known, the calculated value of T may be used. The values of N, $\varepsilon_{14 \text{ MeV}}$ and ε_{Cf} are obtained from experiments in the "boron tank", and that of N_{sec}, from expression (1).

2.   DESCRIPTION OF THE EXPERIMENTAL SET-UP

The experimental facility consists of an NG-150 M neutron generator with a modernized ion conductor and a total neutron absorption detector (TAD) (Fig. 1). The ion conductor is about 1 m long, in order that the ion beam may be directed to the target located at the centre of the TAD. It consists of a thin-walled, non-corroding tube of varying cross-section. The wall thickness is 0.5 mm. The target unit is of simplified design in order to reduce neutron scattering on its components to a minimum. The TiT target, 2, on a copper base is cooled by water. The diameter of the target is 28.5 mm, the thickness of the base is 0.7 mm. The thickness of the layer of water cooling the target is 1.5 mm, the diameter of the beam to the target does not exceed 15 mm. A DKPs-25 surface-barrier counter [6] is positioned at an angle of nearly 180° to the deuteron beam for recording accompanying α-particles from the T(d,n)α-reaction. The parameters of the counter are: U_{opt} = 15 V, the energy resolution = 33 keV, the thickness of the sensitive layer is 89 μm. The area of the counter diaphragm is 7.14 mm^2. It is covered with an aluminium foil 3 μm thick. The foil cuts out the scattered deuterons, thanks to which the counter is not overloaded, and the α-particles, having an energy of 3.6 MeV, penetrate it unhindered, but in this process they are partially slowed down. A foil 3 μm thick was chosen so that on the analyser's scale it would be possible to resolve pulse peaks originating with α-particles from the T(d,n)α-reaction and with D(d,p)T protons; from these peaks [17], the fraction of neutrons from the D(d,n)^{3}He reactions in the spectrum of the source can be estimated. The total neutron absorption detector is a spherical layer, filled with a solution of boric acid in distilled water. The boric acid is 86.6% enriched in the isotope ^{10}B. The concentration of boron-10

nuclei in the "boron tank" is 7.95×10^{19} nuclei/cm^3. The outer spherical shell of the TAD, with a diameter of 1360 mm, is made from a 2 mm sheet of brass. The inner shell, 2.0 mm thick, is made of stainless steel and has a diameter of 400 mm. The surface of the inner shell, on the side facing the air-filled cavity, is covered with a layer of cadmium 1 mm thick.

Cadmium is essential for preventing the outflow of thermal neutrons into the assembly under study. In the inner cavity of the TAD, formed by the inner spherical shell, a simplified support is positioned beneath spherical samples of different diameters. The support is made of aluminium and is adjustable in height. The inner shell with the support and spherical assembly is attached to a hollow cylindrical mounting made of aluminium. The cavity inside the mounting is filled with a boric acid solution. This entire structure, including the external spherical shell, is fastened to a mobile mounting which is able to move in the direction of the deuterium beam of the neutron generator. In the vertical surface passing through the centre of the TAD, there are radial channels for accommodating the boron counter. The channels are at angles of 0°, 40°, 80°, 120° and 140° to the deuteron beam. This arrangement of the channels is dictated by the need to allow for the kinematics of T(d,n)α-reaction, in which the neutrons are dependent both on the energy and angle of emission and also on the azimuthal angle Θ. The channels are filled from thin-walled aluminium tubes; D_{int} = 18 mm, D_{ext} = 20 mm. Unlike the hollow channel in the case of the ion conductor, the channels are filled with a boric acid solution. A standard boron counter KNT-10 (1) is used for the measurements. The diameter of the counter is 7 mm, its length 70 cm. The boron layer is 5 mm long. The distance between the centre of the boron chamber and its rear part is 31 mm. The chemical composition of the radiator is amorphous boron; its density is 0.5 mg/cm^2. The counter is joined hermetically to a thin, hollow rod 4 mm in diameter and inside which a signal cable is inserted. By means of the rod, the counter is moved along the channel. The feed voltage of the counter is +500 V, which corresponds to a plateau in the counting characteristic. The position of the counter is measured by means of a ruler with a scale value of 1 mm. In order that the boron layer of the counter may be placed at any point along the radius of the TAD, recesses 33 mm long and 9 mm in diameter were made in the region of each experimental channel in the inner spherical shell for accommodating the rear part of the boron counter in the measurement at points not far from the inner shell of the spherical layer of the TAD.

In the boric acid solution, at an angle of 90° to the deuterium beam, at a distance of 210 mm from the centre of the TAD, there is a standard fission chamber KNT-5 (7) serving as a neutron yield monitor.

Lead and bismuth assemblies of four spherical shapes were studied by means of the TAD. They consisted of two hemispheres. Each assembly had a channel 50 mm in diameter for placement in the centre of the neutron generator target. The assemblies in the inner cavity of the TAD were mounted coaxially with the ion conductor channel. The dimensions of the assemblies studied are given in Table 3.

3   EXPERIMENTAL TECHNIQUE

3.1   Determination of the value of ε_{14} MeV

To determine ε_{14} MeV, it is necessary to measure the absolute strength of the 14 MeV source. To this end, the measuring system comprising a target, a diaphragm and an alpha-counter was calibrated by means of a ^{238}Pu alpha source from an OSAI set. The main characteristics of the reference α-source are given in Table 4. At the time of measurement, the strength of the source has 2.26 x 10^4 α-particles/s at a 2π angle. The source was mounted at the site of the TiT-target in the ion conductor. Ten measurements were made, each of them lasting $\sim$ 10h. During this time $\sim$ 1200 pulses accumulated in the peak. Averaged over the 10 measurements, the α-particle counting rate of the counter was 126.45 pulses/h. Let us find the number of neutrons emitted by the neutron generator target for one α-counter pulse:

$$X \frac{neutr.}{\alpha\text{-part.}} = \frac{2.2,26\ 10^4\ neutr./s\ 3,6.\ 10^3 s}{1,05.126,45\alpha\text{-part.}} = 0,1226.10^7\ neut./\alpha\text{-part.}$$

Here (2 x 2.26/1.05) x 10^4 neutr./s in 4π is the strength of the neutron source, which give the same pulse count in the peak from α-particles as an alpha source with an emission rate of 2.26 x 10^4 α-part./s in 2π; 1.05 is the anisotropy factor of neutron emission from the target, corresponding to an angle of 175° and of 100 keV deuteron energies, to the deuteron beam, under which the α-counter was mounted.

The anisotropy factor varies slightly with changes in deuteron energy. To obtain the strength of the 14 MeV neutron source, it is sufficient to multiply the value of X, neutr./α-part. by the area of α-pulse peak. The average strength of the 14 MeV neutron source during the time of operation is 3 x 10 neutr./s. The energy of the α-particles of a standard source is higher than that of the α-particles escaping from the TiT-target. To have the assurance that, despite the difference in α-particle energy, the calibration is still correct a supplementary experiment was set up in which the thickness of the aluminium foil was increased to 4 μm. The count rate at the peak of the alpha particles from the TiT-target and the KNT-5 monitor was measured at the same time. The ratios of these two count rates with foils of 4 and 3 μm thickness on the α-counter diaphragm were consistent within the limits of measurement errors. This is evidence that the value of X, neutr./α-part. obtained for α-particles of the reference source is also correct for the α-particles escaping from the TiT-target.

To measure ε_{14} MeV, the TAD was moved into the ion conductor of the neutron generator in such a way that the target was located in the centre. The spherical layer of the TAD was then filled with a solution of boric acic. The KNT-5 monitor was calibrated for one α-counter pulse. For this purpose, when the neutron generator was switched on,

measurements were performed simultaneously over two circuits: the α-counter and the KNT-5 monitor. The counting time at each point was 100 s. Figure 3 showns diagrams of the measurement circuits. The accelerating voltage of the neutron generator during operation was ~ 115 kV.

The characteristic shape of the spectrum of pulses emitted by the neutron generator, obtained on the analyser scale, is shown in Fig. 2. The dual peaks from the α-particles and the protons (owing to the D^+ and D^{2+} beam components) can be seen clearly here. The peaks from the α-particles are located further to the left of the proton peaks, since the α-particles, in contrast to the protons, definitely release energy on to the aluminium foil of the diaphragm. The areas of the α-particle and proton peaks were obtained by summing over the channels. The peak from the protons gives an idea of the proportion of neutrons from the $D(d,n)^3He$-reaction. Calibration was performed twice: before and after measurement on the TAD. The results were averaged for the two series. During operation, the contribution from $D(d,n)^3He$-neutrons showed practically no change remaining at a level of 1%. The α-counter from the ion conductor was then removed so as to avoid its failure due to limited service life. After this a measurement was made of the spatial distribution of the count rate of the KNT-10 boron counter per one reference count of the KNT-5 monitor. The arrangement of the KNT-10 measurement circuit is shown in Fig. 3. The two circuits, KNT-5 and KNT-10 were switched on simultaneously with the neutron generator. The measurements were made in five channels, at angles of 0°, 40°, 80°, 120° and 140° to the deuteron beam. In each channel the measurements were carried out at 15 points along the radius, three times each at each point. The measuring time at each point was 30 s. The results of the measurements are shown in Table 5. The ratio of the KNT-10 and KNT-5 count rates was integrated numerically over the volume of the TAD according to the expression

$$ I = \sum_j (r_{j+1}^3 - r_j^3) \sum_i f_{ij}(\cos\theta_i - \cos\theta_{i+1}) . $$

where 1 is the integral of the ratio of the KNT-10 and KNT-5 count rates over the volume of the TAD; r_j is the distance to the centre of the TAD; θ_1 is the azimuthal angle with the direction of the deuteron beam; f_{ij} is the count rate of the boron counter per one KNT-5 reference count at the measurement point. (In the measurements on the ^{252}Cf source f_{ij} is the count rate of the boron counter at the point of measurement.)

Knowing the integral 1, the KNT-5 count rate calibration factor for one α-particle, recorded as the α-counter Y, α-part./count KNT-5, and also the value of X; neutr./α-part., we can obtain $\epsilon_{14\ MeV}$.

$$ \epsilon_{14MeV} \cdot \frac{KNT-10\ count}{neutr.} = \frac{I, \dfrac{KNT-10\ count}{KNT-5\ count}}{X, \dfrac{neutr.}{\alpha\text{-part.}} \quad Y, \dfrac{\alpha\text{-part.}}{KNT-5\ count}} $$

Numerically, ϵ_{14MeV} = 0,0911 ± 0,0023.

3.2 Determination of ε_{Cf}

A standard ^{252}Cf source with a yield of 6.286 x 10^7 neutr./s (at the time of measurement) was used as a source of simulating secondary neutrons. The error in determining the strength of the source was 3% for a confidence coefficient of 0.95. The source parameters are shown in Table 6. A source on a special rod was introduced into the centre of the TAD through the channel for the ion conductor. Next, the spatial distribution of the KNT-10 count rate was measured at the same points in space as in the measurement of $\varepsilon_{14\ MeV}$. For distances greater than 10 cm from the inner shell of the TAD, the exposure was equalized 10s. For distances greater than 10 cm, the exposure varied from 300 s to 1 h. Table 7 presents the results of measurements with a ^{252}Cf source, these being reduced to a single 100-second exposure. The integral, referred to the strength of the source, represents the value of ε_{Cf} which is being sought. The numerical value obtained for ε_{Cf} was 0.09977 ± 0.0015.

3.3. Determination of absolute neutron leakage M in lead and bismuth assemblies in terms of one 14-MeV neutron

The values of the N count rate of a boron counter integrated over the volume of a TAD for each assembly studied, in terms of one 14 MeV source neutron, were obtained in the same way as the value of $\varepsilon_{14\ MeV}$. For each assembly we determined its calibration factor Y, α-part./count for KNT-5 and the integral 1, and count KNT-10/count KNT-5. The results of the experiments for assemblies of lead and bismuth are presented in Tables 5-11. Also presented here are the KNT-5 calibration factors for an α-counter in a "boron tank" with lead and bismuth assemblies with a 14-MeV source and in a "boron tank" with a 14-MeV neutron source without assemblies (Table 12).

Each calibration coefficient Y, KNT-5 α-part./count was averaged over 14 experiments (7 each in a fresh target and 7 after work with it). In the transition to a new assembly, a new target was installed. The value T for lead was taken from a calculation according to the BLANK program. It is in good agreement with earlier measurements on transmission [18-20]. The results obtained in these studies and also the BLANK program calculations are presented in Fig. 4.

The value of T for bismuth was calculated by using the cross-section for total inelastic interaction taken from the paper of Graver and Davir [19], according to the expression $T = e^{-\Sigma x}$ (x is the thickness of the multiplier layer; Σ is the macro cross-section of the inelastic interaction). This expression does not take into consideration the fact that elastically scattered neutrons can interact inelastically with nuclei of the assembly and reduce the contribution to T. Nevertheless, the value of T calculated in this way is consistent with the results of Refs [8, 19, 21] presented in Fig. 5. From equations (1) and (2) we find the leakage of neutrons:

$$M = T + \frac{N - \varepsilon_{14\ MeV}\ T}{\varepsilon_{Cf}}$$

The errors in the values obtained experimentally were calculated accoring to the expression:

$$\sigma_y = \sqrt{\sum_i (\partial y/\partial x_i)^2 \sigma_{x_i}^2} \ .$$

where y is the value sought for; σ_y is the mean square error of the required value; x_i is a parameter for determining the required value; σ_{x_i} is the mean square error of the parameter used.

For the mean square error of transmission, σ_T, we used the statistical calculation error obtained as $\sqrt{T}/N'$, where T is the neutron transmission and N' is the number of histories in the calculation by the Monte Carlo method.

4.   COMPARISON OF EXPERIMENT AND CALCULATION

The experimental values for neutron leakage in the case of spherical assemblies made of lead and bismuth, and also the calculated values and the experimental data on N_{sec} are given in Table 13. The experimental values of M and N_{sec}, adjusted to the value of the fraction of neutrons from the $D(d,n)^3He$-reaction, which is equal to $\sim$ 0.01 (in terms of one 14-MeV neutron from the source). The errors are listed for a 68% confidence interval.

The calculation was made in accordance with the BLANK program, by the Monte Carlo method. The constants for lead from the ENDL library were used in the calculation. Since there were no constants in the library for leakage from bismuth assemblies, they were not calculated. It will be seen from Table 13 that the calculation based on a value of 0.065 ± 0.035 for 3 cm and on a value of 0.08 ± 0.047 for 9 cm in the case of lead assemblies underestimates the leakage of neutrons. This result correlates with those of Refs [10, 12, 13], although the leakage values obtained are not as high as those of Takahashi et al. [13] and are found to be closer to the calculated value. The main reason for the discrepancy found between experiment and calculation can be considered the underestimation of the cross-section for the (n,2n) reaction in the calculation by the BLANK programs. The considerable difference between calculation and experiment found by Zagryadskij et al. for indium and radium detectors cannot be explained solely by the difference in the cross-section for the (n,2n) reaction (as follows from the present experiment). The main reason for this difference lies in the harder - by comparison with calculation - real spectrum of secondary neutrons and the greater sensitivity of these detectors to the shape of the secondary spectrum and to the secondary neutron flux, by comparison with what is found for the TAD.

CONCLUSIONS

1. The "boron tank" method was used to obtain values for neutron leakage and the number of secondary neutrons per one 14-MeV neutron from a source, in the case of lead and bismuth assemblies with multiplication zones 3 cm and 9 cm in thickness. It is shown experimentally that the lead and bismuth zones, which are ~ 10 cm thick, are sufficient for the multiplication of fusion neutrons by a factor of one-and-a-half.

2. The difference between experimental and theoretical results for lead assemblies exceed the errors of the experimental values by a factor of 1.6 and, for the zones 3 cm and 9 cm thick, by a factor of 1.7. These differences show that in the calculation by the BLANK program, the cross-section for the (n,2n) reaction in lead is underestimated. An increase in the cross-section for this reaction relative to the one adopted in the ENDL library can be recommended.

3. The results obtained warrant the conclusion that the difference between calculation and experiment for the measurement of spectral indices in lead as given by Ref. [16] are due mainly to the harder - by comparison with calculation - real spectrum of secondary neutrons in lead.

REFERENCES

[1]   Vasil'ev, V.G. et al., Blanket for tritium production with continuous sampling in the INTOR facility. In "Questions of atomic science and technology". Series: thermonuclear fusion, Vol. 1(7) (1981) 77 (in Russian).

[2]   Sakin S. A neutron physics analysis for the experimental facility LOTUS. Atomkernenergie-Kerntechnick, 1982, vol. 41 (2), p. 95 — 98.

[3]   Conn R.W. et al. Fusion-Fision hybrid design with analysis of direct enrichment and non-proliferation features. (The SOLASE-H study).— Nucl. Eng. Des., 1981, vol. 63, p. 357.

[4]   Youssef M.Z. et al. Impact of cross-section uncertainties on the nuclear design of hybrid reactor. — Nucl. Tech. Fusion, 1982, vol. 2, p. 649 — 666.

[5]   Adam A. et al. The mechanism of the (n, 2n) reaction. — Nucl. Phys., 1963, vol. 49, p. 489.

[6]   Bödy Z.T., Csikai J. Recommended valnes of (n, 2n) crass-section at 14 MeV. — Atom. Energy Rev., 1973, vol. 11, p. 153 — 165.

[7]   Akiyoshi et al. Inelastic scuttering of 14 MeV neutrons by heavy nuclei. — J. Nucl. Sci. Tech., 1974, vol. 11, p. 523 — 534.

[8]   Frehant, J., Mosinski, G., Measurement of (n,2n) and (n,3n) cross-sections between the threshold and 15 MeV by the liquid scintillation fat method. In Neutron Physics, Proceedings of the Third All-Union Conference on Neutron Physics, Kiev, 9-13 June 1975. Moscow, 1976, No. 4, p. 303 (in French/Russian).

[9]   MacGregor M.N., Ball W.R., Booth R. Nonelastic neutron cross sections at 14 MeV.— Phys. Rev., 1956, vol. 108, N° 3, p. 726 — 734.

[10]   Aleksandrov, V.V. et al., Experimental study of the neutron spectrum in lead, with neutron sources of 14-MeV energy. Atomnaya Ehnergiya 52/6 (1982) 422 (in Russian).

[11]   Marin, S.V., Markovskij, D.V., Shatalov, G.E., IAEh-2382 preprint, Moscow (1977) (in Russian).

[12]   Bogomolov, A.M. et al., Study of the transfer of 14-MeV neutrons in a
        mock-up of a thermonuclear reactor shield, Preprint IAEh-4030/8, Moscow
        (1984).

[13]   Takahashi A. et al. Proc. 12th SOFT Symp. on fusion technology.
        Jülich, Sept., p. 687, 1982, Pergamon Press, Oxford.

[14]   Segev M. Analysis of (n, 2n) multiplication in lead. — Annals of
        Nucl. Energy, 1984, vol. 11, N° 4, p. 153 — 205.

[15]   Konatov, S.D., Novikov, V.M., Chuvilin, D.Yu., Criteria for the
        selection of activation detectors for integral experiments with a
        14-MeV neutron source. Preprint IAEh-3989/4, Moscow (1984) (in
        Russian).

[16]   Zagryadskij, V.A. et al., The total absorption method in the
        measurement of multiplication factors in 14-MeV neutrons, IAEh preprint
        4171/8, Moscow (1985) (in Russian)

[17]   Ramendit, Z.A., Study of methods of determining flux density in
        carrying out a reaction, Izmeritel'naga tekhnika 6 (1981) 61 (in
        Russian).

[18]   Taylor H.L., Lönsjo O., Bonner T.W. Nonelastic scuttering cross-
        section for fast neutrons. — Phys. Rev., 1955, vol. 100, N° 1,
        p. 174 — 180.

[19]   Graver E.R., Davir R.W. Cross-sections for nonelastic interaction
        of 14 MeV neutrons with varions elements. — Phys. Rev., 1955,
        vol. 97, N° 5, p. 1205 — 1212.

[20]   Hansen L.F. et al. The transport of 14 MeV neutrons through heavy
        materials, 150 ≤ A ≤ 208. — Amer. Nucl. Soc., 1981, vol. 38, p. 567 —
        568.

[21]   Phillips D.D., Davis R.W., Gaver E.R. Inelastic collision cross-section
        for 14-MeV neutrons. — Phys. Rev., 1952, vol. 88, N° 3, p. 600 — 603.

Table 1. Cross-section of the (n, 2n) reaction for
14-MeV neutrons for lead and bismuth
according to various sources in the literature

Element	E = 14 Mev, mb	Reference
Pb	1800 ± 200 1953 ± 157 2130	[5] [6] [7]
Bi	1950 ± 80 2214 ± 100 2250 ± 140 2340 2560 ± 40	[5] [6] [8] [7] [9]

Table 2. Experimental and theoretical leakage of neutrons from lead spherical shells
in terms of one 14-MeV neutron from a source [13]

Energy range, MeV	Library	б, см			
		3	6	9	12
0,3 − 15	Experiment	1,22 ± 0,01	1,41 ± 0,01	1,59 ± 0,03	1,60 ± 0,09
	NITRAN (S19), ENDF/B-IV	1,124	1,214	1,27	1,296
	ANISN (P5 S16), ENDF/B-III	1,131	1,234	1,309	1,359
4,0 − 15	Experiment	0,80 ± 0,01	0,65 ± 0,02	0,54 ± 0,03	0,41 ± 0,02
	NITRAN (S19), ENDF/B-IV	0,756	0,599	0,468	0,363
	ANISN (P5 S16), ENDF/B-III	0,774	0,627	0,502	0,401
0,3 − 4,0	Experiment	0,42 ± 0,01	0,76 ± 0,01	1,05 ± 0,01	1,19 ± 0,09
	NITRAN (S19), ENDF/B-IV	0,365	0,614	0,800	0,932
	ANISN (P5 S16), ENDF/B-III	0,356	0,606	0,805	0,957

Table 3. Dimensions of lead and bismuth assemblies

No. of assembly	Pb		Bi	
	R_{int} , CM	R_{ext} , CM	R_{int} , CM	R_{ext} , CM
1	9,15	12	9,15	12
2	3	12	3	12

Table 4. Characteristics of reference spectrometric ^{238}Pu source

$T_{1/2}$, years	Value of α-part. flux at 2π angle, α-part./s	Value of source activity decays/s	Relative error, %	Value of the energy of α-particles of principal transitions, in MeV
87,74	2,26.10⁴	4,50.10⁴	± 2	5,49
				5,15

Table 5. Spatial distribution of the ratio of the count rate of the KNT-10 to that of the KNT-5 in the total absorption detector (TAD), for a neutron source with 14-MeV energy, without experimental assemblies

R, CM	θ, degrees				
	0	40	80	120	140
0	21,01	20,18	19,81	20,19	19,40
1	31,87	30,08	29,07	29,00	28,89
2	36,95	35,38	32,86	33,19	33,06
3	39,534	35,67	33,48	34,02	34,67
4	37,82	35,24	32,47	34,281	33,46
5	36,60	34,05	31,38	31,15	31,73
6	32,89	30,94	27,97	30,33	26,21
8	28,30	25,70	23,52	24,43	24,92
10	23,01	21,50	19,44	20,09	20,79
14	16,25	14,87	13,26	14,35	13,77
20	9,11	8,61	7,93	8,11	7,92
25	5,88	5,72	5,05	5,07	5,08
30	3,75	3,66	3,17	3,18	3,24
35	2,36	2,30	2,02	2,06	2,02
40	1,42	1,40	1,31	1,28	1,23

Note: In tables 6 and 8-11, θ is the azimuthal angle to the direction of the deuteron beam, R is the distance from the inner shell of the TAD to the measurement point (centre of the KNT-10 boron layer).

Table 6. Parameters of the reference ^{252}Cf source

Neutron yield at 4π agle, neutr./s	Error, measured with a confidence interval of 0,95, %	$T_{1/2}$, years	Ampoule material	Ampoule diameter, mm	Ampoule height, mm
$6,2276.10^7$	3	2,638	12X18H10T	7	14

Table 7. Spatial distribution of the KNT-10 count rate in the total absorption detector (TAD) for a ^{252}Cf neutron source

R, cm	θ, degrees				
	0	40	80	120	140
0	4211	4115	4371	4088	4271
1	6344	6150	6538	6294	6401
2	7205	7105	7379	7055	7259
3	7278	7138	7403	7159	7426
4	6790	6719	6987	6741	6912
5	6090	5908	6246	5988	6225
6	5246	5146	5378	5154	5382
8	3671	3532	3765	3692	3735
10	2494	2414	2604	2460	2498
14	1073	1019	1136	1056	1118
20	316,7	305,7	334,7	309,7	321,3
25	121,5	116	124,3	122,7	124,9
30	50,08	49,7	50,7	47,3	52,5
35	23,32	22,2	24,3	22,5	24,5
40	10,8	11,2	10,8	9,53	11,8

Table 8. Spatial distribution of the ratio of the count rate of the KNT-10 to that of the KNT-5 in the TAD for a lead assembly with a zone thickness of 3 cm

R, cm	θ, degrees				
	0	40	80	120	140
0	22,84	21,31	21,646	21,06	21,55
1	33,55	31,07	32,954	30,58	31,79
2	39,07	36,40	36,67	35,34	36,49
3	39,06	36,91	35,90	35,33	37,06
4	37,12	34,42	34,36	32,87	34,62
5	33,37	31,71	30,37	30,42	30,58
6	29,29	27,78	26,65	26,17	27,71
8	22,44	20,78	20,25	19,87	20,01
10	15,99	15,08	14,81	14,78	14,95
14	9,11	8,45	8,43	8,42	8,33
20	4,32	4,16	4,12	3,93	3,96
25	2,61	2,53	2,33	2,33	2,37
30	1,59	1,60	1,47	1,45	1,45
35	0,992	0,941	0,910	0,909	0,893
40	0,599	0,59	0,530	0,502	0,529

Table 9. Spatial distribution of the ratio of the count rate of the KNT-10 to that of the KNT-5 in the TAD for a lead assembly with a zone thickness of 9 cm

R, cm	θ, degrees				
	0	40	80	120	140
0	23,50	22,46	22,753	21,35	22,74
1	34,82	33,15	33,225	32,27	33,38
2	39,11	37,47	36,73	35,82	37,86
3	38,92	37,98	37,21	36,95	38,19
4	36,10	35,09	34,44	33,71	35,09
5	32,75	30,14	30,05	30,07	31,19
6	27,84	26,13	25,98	25,48	26,75
8	19,32	18,32	17,78	18,00	18,49
10	12,62	12,03	11,97	11,89	12,53
14	5,75	5,39	5,41	5,53	5,86
20	2,13	2,07	2,00	2,05	2,27
25	1,13	1,08	1,07	1,06	1,15
30	0,628	0,618	0,621	0,612	0,660
35	0,376	0,365	0,347	0,355	0,389
40	0,226	0,215	0,190	0,207	0,227

Table 10. Spatial distribution of the ratio of the count rate of the KNT-10 to that of the KNT-5 in the TAD for a bismuth assembly with a zone thickness of 3 cm

R, cm	θ, degrees				
	0	40	80	120	140
0	21,33	20,73	21,09	20,08	20,46
1	31,17	31,21	31,49	30,98	30,81
2	36,78	35,38	35,921	34,38	34,88
3	38,13	35,88	35,832	35,11	36,10
4	35,46	33,45	33,17	32,27	34,22
5	32,30	31,65	30,41	29,27	29,82
6	29,03	27,00	27,36	26,33	27,17
8	21,4	20,40	20,50	20,75	20,30
10	16,06	15,47	15,04	14,91	15,20
14	9,11	8,59	8,27	8,68	8,75
20	4,41	4,29	4,19	4,15	4,20
25	2,69	2,59	2,521	2,59	2,50
30	1,63	1,61	1,56	1,50	1,50
35	1,00	0,982	0,947	0,943	0,933
40	0,62	0,596	0,560	0,544	0,53

Table 11. Spatial distribution of the ratio of the count rate of the KNT-10 to that of the KNT-5 in the TAD for a bismuth assembly with a zone thickness of 9 cm

R, cm	θ, degrees				
	0	40	80	120	140
0	23,02	22,24	22,26	21,10	22,30
1	35,97	34,21	33,85	31,41	33,52
2	40,00	37,88	36,93	36,17	37,92
3	39,95	37,61	36,31	35,40	37,68
4	36,82	35,31	34,46	32,92	34,83
5	33,46	31,02	30,68	29,09	30,31
6	29,03	26,93	28,16	25,32	26,54
7	20,47	18,91	18,78	17,88	18,49
8	14,11	13,08	12,72	12,51	12,68
10	6,34	5,83	5,98	5,79	5,93
14	2,47	2,35	2,29	2,23	2,30
20	1,29	1,26	1,24	1,22	1,22
25	0,736	0,727	0,694	0,671	0,703
30	0,458	0,439	0,427	0,409	0,422
35	0,27	0,262	0,250	0,244	0,249

Table 12. Calibration factors of the KNT-5 for the α-counter Y, α-part/count KNT-5 for the 14 MeV source of lead and bismuth assemblies

Source with 14-MeV neutron energy	Lead assembly $\delta = 3$ см	Lead assembly $\delta = 9$ см	Bismuth assembly $\delta = 3$ см	Bismuth assembly $\delta = 9$ см
54,725 ± 0,448	28,322 ± 0,131	17,782 ± 0,125	29,438 ± 0,138	18,286 ± 0,139

Note: δ = thickness of multiplier layer

Table 13. Experimental and calculated values of absolute leakage, number of secondary neutrons, calculated values of the transmission function of 14-MeV source neutrons for lead and bismuth assemblies, in terms of one 14-MeV source neutron

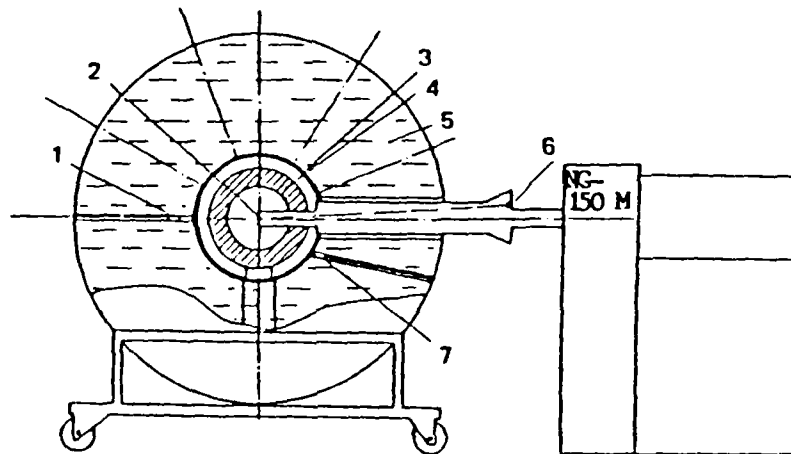| Material and thickness of assemblies	Transmission function, T (calc.)	Absolute leakage, M (calc.)	Absolute leakage, M (exper.)	No. of secondary neutrons (calc.)	No. of secondary neutrons (exper.)
Pb, $\delta = 3$ см	0,749	1,193	1,258 ± 0,037	0,444	0,509 ± 0,036
Pb, $\delta = 9$ см	0,447	1,449	1,529 ± 0,045	1,002	1,083 ± 0,045
Bi, $\delta = 3$ см	0,807	—	1,260 ± 0,038	—	0,453 ± 0,036
Bi, $\delta = 9$ см	0,526	—	1,557 ± 0,045	—	1,031 ± 0,045

—

Fig. 1. Diagram of the total neutron absorption detector (TAD):
1 – KNT–10; 2 – target; 3 – cadmium shield;
4 – the assemblies under study; 5 – $H_3^{10}BO_3$ solution;
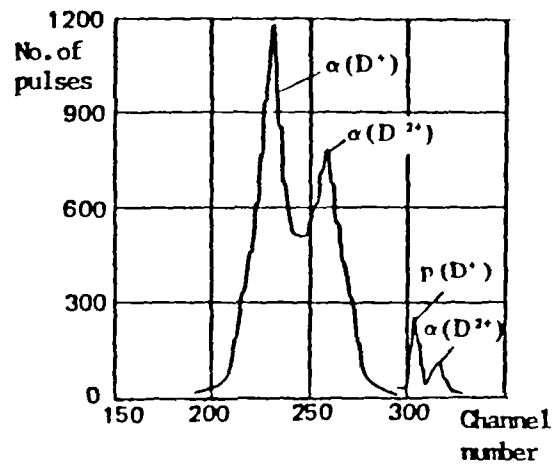6 – DKPs –25 α–counter; 7 – KNT–5

Fig. 2. Spectrum of particles emitted by the TiT–target
of the neutron generator

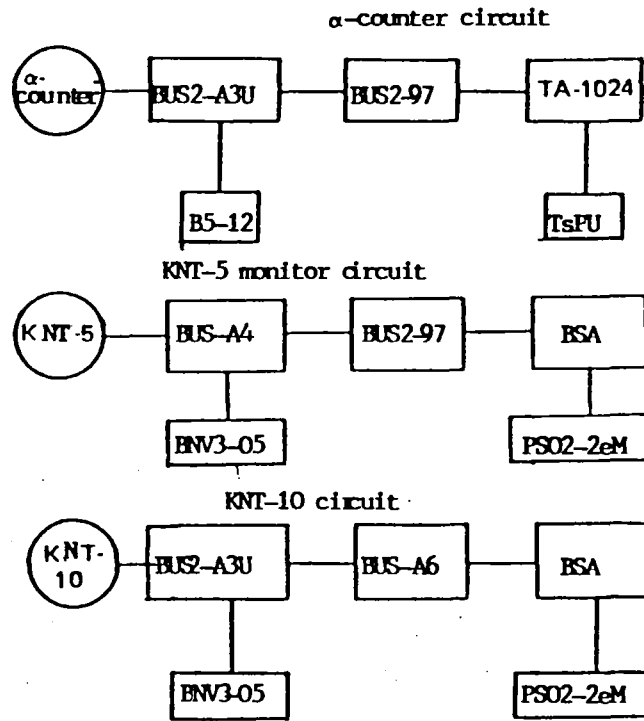α-counter circuit

KNT-5 monitor circuit

KNT-10 circuit

Fig. 3. Block diagram of measurement circuits
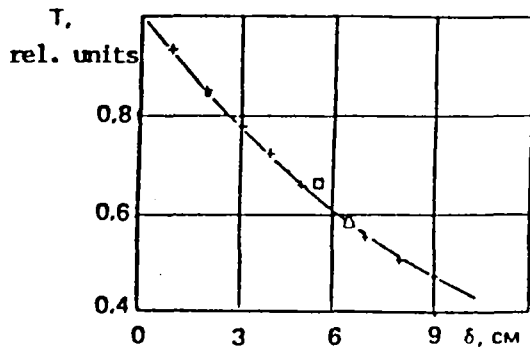
Fig. 4. Transmission function, T, of 14-MeV neutrons, for spherical lead shells of thickness δ [18 (○), 19 (△), 20 (□)], calculated according to expression [x]

$$e^{-\Sigma_{nel} r} \quad (+) \quad [\sigma_{nel} = 2,5 \; \delta;$$

$$\rho = 3,3.10^{22} \; nuclei/cm^3]$$

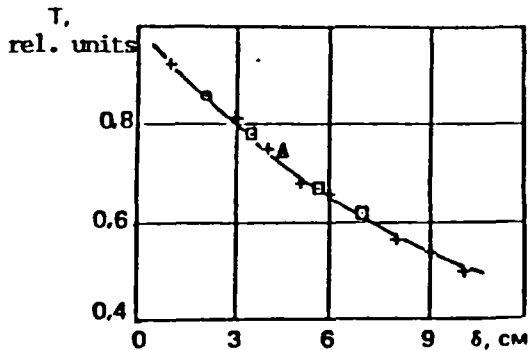**Fig. 5.** Transmission function, T, of 14 MeV neutrons, for spherical bismuth shells of thickness δ [18 (○), 19 (△), 21 (□)], calculated according to expression [x]

$$e^{-\Sigma_{nel} r} \quad (+) \quad [\sigma_{nel} = 2,54 \; \delta;$$

$$\rho = 2,81.10 \; nuclei/cm^3]$$